Chemical Engineering Journal 545 (2026) 179368

Contents lists available at ScienceDirect

Chemical Engineering Journal

journal homepage: www.elsevier.com/locate/cej

Oscillatory motion of trickle-bed reactor can break up liquid channeling and thus increase reaction efficiency

Bilge Su Subasi [a], Triani Nur Zahra [b], Andreas Bösmann [a], Robinson Perić [b,*], Peter Wasserscheid [a,c,d], Moustafa Abdel-Maksoud [b]

[a] Friedrich-Alexander University, Lehrstuhl für Chemische Reaktionstechnik, Egerlandstraße 3, Erlangen, 91058, Bavaria, Germany
[b] Hamburg University of Technology, Institute for Fluid Dynamics and Ship Theory, Am Schwarzenberg-Campus 4, Hamburg, 21073, Germany
[c] Forschungszentrum Jülich GmbH, Helmholtz-Institute Erlangen-Nürnberg for Renewable Energy (IET-2), Cauerstraße 1, Erlangen, 91058, Bavaria, Germany
[d] Forschungszentrum Jülich GmbH, Institute for a Sustainable Hydrogen Economy (IHE), An der Deutschen Welle 7a, Jülich, 52428, Bavaria, Germany

ARTICLE INFO

Dataset link: https://doi.org/10.5281/zenodo.19662048

Keywords:
Trickle-bead reactor
Oscillating reactor
Liquid organic hydrogen carrier
Reaction efficiency
Computational fluid dynamics

ABSTRACT

We report that applying an oscillatory pitching motion can substantially increase the reaction efficiency in trickle-bed reactors used for the hydrogenation of liquid organic hydrogen carriers (LOHC). In the present experiments, steady-state reaction was reached 14 times faster and with approx. 25% larger mean efficiency for the pitching reactor compared to the conventional non-moving reactor. Increasing the pitching amplitude from 1° to 4° accelerated the reaction by about 45%. Strong memory effects were observed, with increased reaction efficiency being maintained for 2 h in a non-moving reactor, if the reactor had been operated under oscillatory pitching motion beforehand. Therefore, the present results indicate that substantial efficiency increases do not require continuous oscillations, instead already occasional reactor motions may suffice. We hypothesize that the increase in efficiency is due to breaking-up of liquid channels. Computational Fluid Dynamics (CFD) simulations and cold-flow experiments are reported that strongly support this theory. It is anticipated that the present findings will be applicable to many other types of trickle-bed reactors as well.

1. Introduction

Trickle-bed reactors have been widely used since the 1950s [1,2], particular in chemical processes involving gaseous hydrogen, a liquid and a solid catalyst. Typically, trickle-bed reactors are vertical cylinders filled with the catalyst, e.g. in the form of spheres with diameters substantially smaller than the cylinder diameter (cf. visualizations in Figs. 2–7). At the top of the cylinder, gas and liquid are introduced. Chemical reactions can occur at the wetted catalyst surface. There are various types of trickle-bed reactors, differing in catalyst size, dimensions, flow rates and other parameters. In the following, the reaction of interest will be the storage of hydrogen using a liquid organic hydrogen carrier, denoted 'LOHC hydrogenation' [3].

A key problem with many trickle-bed reactors is the complex fluid dynamics inside the reactor: Small changes in the setup can substantially alter the flow and thus also the reaction speed, often in a seemingly unpredictable manner. Ideally, the reactor would be operated under plug-flow conditions, i.e. uniform flow and wetting throughout the reactor. Then, the reactor typically behaves reproducibly and allows determining reaction kinetics. However, in many applications, plug-flow conditions cannot be realized. For example, low liquid flow rates and low ratios of reactor diameter per catalyst-particle diameter (ca. <25) can cause liquid maldistribution, stagnant fluid, incomplete catalyst wetting and channeling, which denotes fluid flowing preferably through narrow channels. Additionally, wall effects can result in liquid preferably flowing along the cylinder walls. Hence, the majority of the catalyst in the reactor may not be supplied with fresh liquid, substantially reducing the reaction efficiency. A detailed discussion of these effects can be found in review papers [4,5]. Also, memory effects can occur and prevent reproducibility, so that slight changes in the flow history or in the experimental setup can result in different reactor behavior, as will be demonstrated in this work. The hydrogenation of LOHC compounds, both in laboratory and commercial scale, is one application where the aforementioned adverse flow phenomena occur [6–10].

A major challenge concerning the design of trickle-bed reactors is that the flow inside the reactor is usually not known. Detailed visualization of the fluid flow inside the reactor is usually not possible during operation. Even in laboratory experiments, flow visualization is challenging: The catalyst pellets are usually intransparent and prevent visual observation of most of the flow in the reactor. Furthermore,

* Corresponding author.
E-mail address: robinson.peric@tuhh.de (R. Perić).

https://doi.org/10.1016/j.cej.2026.179368
Received 24 April 2026; Received in revised form 1 July 2026; Accepted 10 July 2026
Available online 16 July 2026
1385-8947/© 2026 The Authors. Published by Elsevier B.V. This is an open access article under the CC BY license (http://creativecommons.org/licenses/by/4.0/).

when reaction takes place at high temperatures, insulation around the reactor turns it into a 'black box'. Point measurements by inserting probes are not able to capture the complex flow behavior that can occur, as will be demonstrated in this work. Computational Fluid Dynamics (CFD) simulations have been suggested to study the flow inside the reactor [5]. To correctly capture the flow physics, simplified simulation approaches (e.g. treating the whole reactor as a single phase) are not suitable. Instead, all three phases (gas, liquid, solid) have to be fully resolved. However, the computational cost of such simulations across the whole reactor appears prohibitive: For example, when scaling the present CFD setup from Section 4 to a full reactor, simulating a typical reaction duration of 4 h would require 3000 mio CPU hours. Such a computation would take 11 days on the world's largest supercomputer ('El Capitan', 11.3 mio. CPU cores and accelerators). Because this is not practical, development of efficient CFD simulation techniques for this application is mandatory.

A major topic of current research on trickle-bed reactors is development of load flexible reactors, which enable quick variation of the reaction speed. In particular, such flexibility is necessary when the reactor is powered by renewable energies [11]. Then, the provided electricity can vary strongly with time, so ideally the reactor should adjust the speed of the reaction accordingly. However, classical reactors do not provide this flexibility; they have to operate at design conditions. Therefore, if electricity supply fluctuates, such classical reactors become inefficient, as they either cannot fully consume the available electricity or suffer from long shut-down times. To increase flexibility of trickle-bed reactors (often termed 'process intensification'), several approaches have been proposed, such as unsteady gas/liquid injection, upwards or cyclic flow (cf. recent literature review in [2]). These solutions often require substantial changes in the reactor design, can increase the costs (sometimes substantially) and are not investigated in the present work.

A comparatively rarely studied approach to vary reaction speed is to apply motions to the reactor, without otherwise changing the reactor design. Conventional reactors are installed fixed, so that motions and accelerations acting on the reactor are minimized. If the flow inside the reactor is sensitive to small changes in the setup, one could anticipate that applying motion or acceleration to the reactor during operation could be used to vary the internal flow and hence the reaction efficiency. If the related physics were understood, this would enable installation of such reactors on moving platforms, which could unlock new applications. Section 2 discusses related challenges and prospects based on an example application, i.e. operating a trickle-bed reactor on a floating offshore wind turbine.

In this work, a non-moving vertical reactor and an oscillatory pitching reactor were investigated. *Vertical reactor* here denotes that the reactor is tilted at zero degree from vertical axis, while *stationary tilting* denotes that the reactor is pitched at a constant angle from the vertical axis, by a rotation about its base. On the other hand, *oscillatory pitching motion* denotes that the reactor performs a sinusoidal pitching motion, by rotating about its base with a constant period and fixed amplitude (cf. Fig. 3).

At present, the literature is inconclusive concerning the effect of motions on the performance of trickle-bed reactors. The literature reviews in Refs. [12–14] come to the following conclusions: Stationary tilting of the reactor led to fluid stratification and reduced catalyst bed wetting, and thus decreased efficiency. Translational movements (horizontal and vertical motion) of the reactor had little impact on efficiency in most studies, with a few exceptions. Oscillatory motions (rolling, pitching, and yaw motion) arguably resulted in incomplete wetting, which reduced reaction efficiency, although less so than stationary tilting. Lower frequencies tended to result in greater efficiency reductions. However, experimental data for various reactor diameters and lengths, as well as catalyst bed parameters, are missing. Refs. [13,15] found that oscillatory pitching motion with angles between 5-10° increased reaction speed, while angles up to 5° did not have any significant effect. Oscillatory pitching with amplitudes above 10° has shown a negative effect on reaction performance [13,16,17]. At present, the reasons for these different observations are not clear. In particular, for LOHC hydrogenation, the reaction of interest in this work, the flow inside the reactor and the effect of reactor motions on the flow and on the reaction efficiency are not known.

The *aims of this work* are to investigate the hypothesis that *oscillatory motion of trickle-bed reactors can increase reaction efficiency substantially*, and to *propose explanations for this phenomenon* based on cold-flow experiments and CFD simulations. This will be investigated for LOHC hydrogenation in a trickle-bed reactor of comparable dimensions as in current industrial applications. This work combines laboratory experiments of a hot reactor, subjected either to stationary tilting or to oscillatory pitching motions, with cold-flow experiments for a fixed upright reactor, as well as with CFD simulations of a simplified reactor. Sections 3 and 4 describe the setup for experiments and simulations, followed by the results in Sections 5 and 6 and a discussion of the findings in Section 7.

2. Example application of trickle-bed reactors installed on a moving platform: research project ProHyGen

This section illustrates the aforementioned necessity of research on moving reactors via an example, the research project ProHyGen funded by the German Federal Ministry for Economic Affairs and Energy.

The main idea behind the project is as follows: A major contribution to the overall costs of offshore wind energy is the grid connection. This applies, even though at present most offshore wind farms are built close to the shore (e.g. in Germany within 100 km distance). In Germany, a substantial increase in installed offshore wind energy is intended (by factor seven until 2045, cf. [18]). Therefore, offshore wind farms are expected to move progressively into deeper waters, where floating concepts become the preferred solution because they can be deployed at virtually any water depth. However, the increasing distance from the coast also makes grid connection progressively more expensive. One promising solution to this challenge is to eliminate the need for a grid connection altogether by using the generated electricity directly on-site for the production of green hydrogen.

The joint research initiative ProHyGen aims to develop a floating offshore wind turbine (FOWT) integrated with a hydrogen production system, enabling the combined generation and storage of green hydrogen in remote marine environments, as shown in Fig. 1. FOWTs provide enough space to integrate the necessary process engineering on board, because they usually require a comparatively large floating substructure. Liquid organic hydrogen carriers (LOHCs) are utilized as the transport medium within this process. Thanks to the LOHC technology, hydrogen can be transported under ambient temperature and pressure. Hydrogen can be stored and transported in the liquid form and with the dehydrogenation reaction at the destination, high-purity hydrogen can be released and used [19].

The floating platform is equipped with a wind turbine that generates electricity to drive the electrolysis of desalinated seawater, enabling on-site hydrogen production. The hydrogen is stored onboard within LOHC (hydrogenation). The hydrogenation process is conducted in a trickle-bed reactor located on the platform. Subsequently, the loaded LOHC is transported to shore using shuttle tankers. Onshore, existing storage and transport infrastructure for crude-oil products can be used to deliver the LOHC to customers, such as energy-intensive industries. There, the hydrogen is released within the dehydrogenation process [20].

The ProHyGen concept aims to provide a scalable and cost-effective solution for offshore green hydrogen production by integrating renewable energy generation, safe storage, and established transport logistics [21,22]. A key advantage of this concept is the use of liquid organic hydrogen carriers (LOHCs), which enable the storage and transport of hydrogen under ambient conditions, thereby significantly enhancing safety [23]. Furthermore, the concept allows the existing

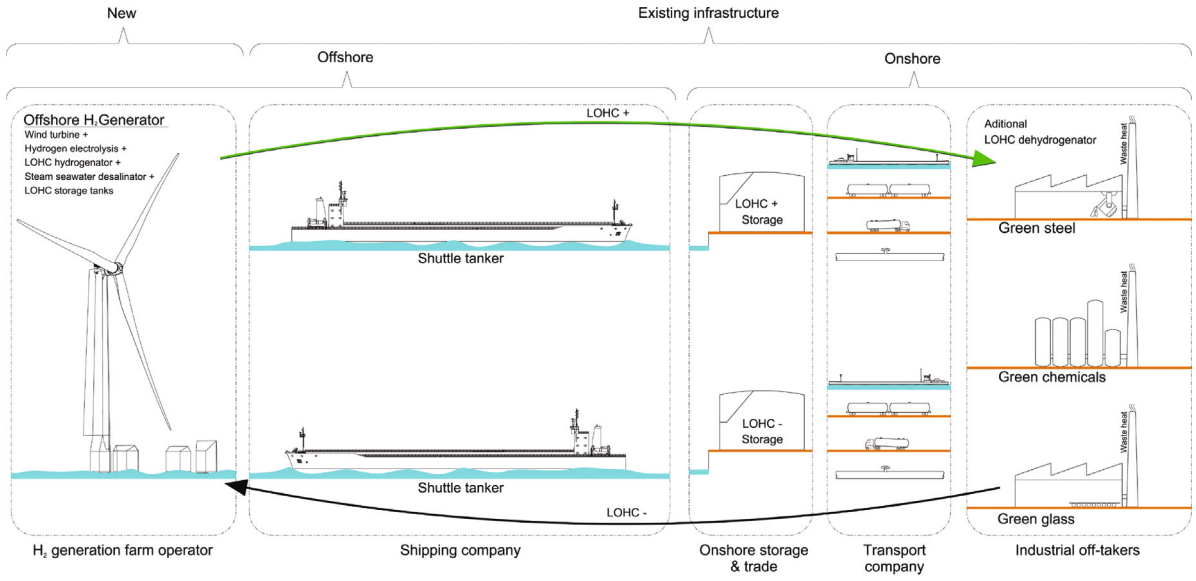

Fig. 1. Visualization of the hydrogen-generation on a floating offshore wind turbine (FOWT), hydrogen-storage within LOHC (denoted 'LOHC+'), transportation of LOHC using existing infrastructure (ships, onshore storage and transport), release of hydrogenation via dehydrogenation process on-site at energy-intensive industries, and return transport of 'unloaded' LOHC (denoted 'LOHC-') back to the FOWT; circular process as developed within the research project ProHyGen.

oil and gas transport infrastructure, including conventional tankers, to be utilized with only minor modifications, substantially reducing both investment costs and operational risks.

Although floating offshore wind turbines (FOWTs) are designed to minimize motions induced by wind and wave loading, they will nevertheless undergo continuous platform motions under realistic environmental conditions. Ocean waves, wind, and currents excite all six degrees of freedom of the floating platform. In the German Exclusive Economic Zone of the North Sea, typical wave periods range from 6 to 8 s, while extreme sea states in the North Atlantic can produce wave periods exceeding 20 s [24]. Consequently, the largest platform accelerations occur predominantly within this period range. Although the mooring system also induces low-frequency motions, the associated accelerations are generally much smaller [25].

The present work therefore investigates how these naturally occurring reactor motions influence the reaction efficiency of trickle-bed reactors.

3. Experimental setup

3.1. Setup overview

Fig. 2 visualizes the experimental setup, which can be divided into three main parts: A *feed delivery system* (from H_2 and substrate tank to the reactor), a *trickle-bed reactor* that can perform pitching motion (gray cylinder and elements connected by horizontal lines) and a *product recovery system* (from V-4 to product tank).

The *feed delivery system* comprised a hydrogen supply line (Air Liquid, quality 5.0) and a liquid benzyltoluene (H0-BT) feed line (Marlotherm® LH Heat Transfer Fluid). During the reaction, the real time hydrogen consumption was measured via the volumetric flow meter (MFM, EL-FLOW/Bronkhorst); the benzyltoluene (H0-BT) amount was controlled via the mini digital mass flow meter/controller (MFC, CORI-FLOW/Bronkhorst) connected to the pump (WADose LITE GEAR/ Flusys).

The reaction took place in a stainless steel *trickle bed reactor* (1.4571, equivalent to AISI 316Ti) with inner diameter 4 cm and inner length 70 cm. The reactor could be tilted or perform oscillatory pitching motions with the help of a motorized arm. The pitch angle was adjusted by changing the attachment point of the arm on the rotating disc (Fig. 3) and the oscillation period (T) was modified by the control panel of a ROTOL 220 G gear motor in conjunction with KIMO MotorMaster MM frequency inverter.

In the trickle-bed reactor, hydrogen was continuously consumed by the reaction and the pressure regulator supplied hydrogen at the same rate as it was consumed, to maintain the operating pressure. The operating pressure in the present experiments was either 20 bar or 30 bar. Hence, no pressure increase occurred during the operations and there was no possibility for gas accumulation. The reactor operated in continuous operation mode, meaning that liquid could continuously leave the reactor and was collected in a separate reservoir (denoted 'cooling coil' in Fig. 2). The reservoir was occasionally emptied by opening valve NC-3, which took roughly 2 min to complete. The opening of this valve resulted in a temporary increase in hydrogen inflow into the reactor, which caused the spikes in the DoH-curves seen in Fig. 8. In this manner the pressure remained constant in the reactor. Therefore, the liquid did not accumulate in the reactor and the setup was comparable to industrial LOHC reactors, except for lower LOHC flow rates and lower amount of catalyst inside the reactor. These two modifications were made to study reactors at DoH-values below 100%. Thus, the DoH-value could be used as an indicator of reaction efficiency.

The samples were collected using valve-5 (V-5), which was directly connected to the reactor. Valve-19 (V-19) and valve-20 (V-20) were used to follow the level of liquid inside the reactor during the flooding operation. The reactor was heated using three electrical heating units (TIC-01, TIC-02 and TIC-03), while the system pressure was controlled by a pressure regulator (PR-1). The temperatures and pressure were monitored using sensors (TIR-01, TIR-02 TIR-03 and PIR-01) mounted on the reactor.

The catalyst bed consisted of a commercial EleMax H101 catalyst from Clariant (Pd/Pt supported on Al_2O_3 pellets (charge DER0015258), which was diluted with different sizes of glass beads. Two different catalyst packings were used, denoted P1 and P2. In P2, substantially less catalyst was used to achieve lower DoH values and to more clearly observe the influence of reactor motion on reaction efficiency. Fig. 4 and Table 1 illustrate the difference.

In the *product recovery system*, the outlet flow went directly to the cooling line, which was connected to the liquid level controller sensors. When the liquid level in the cooling line reached LI-2 (Sensor:

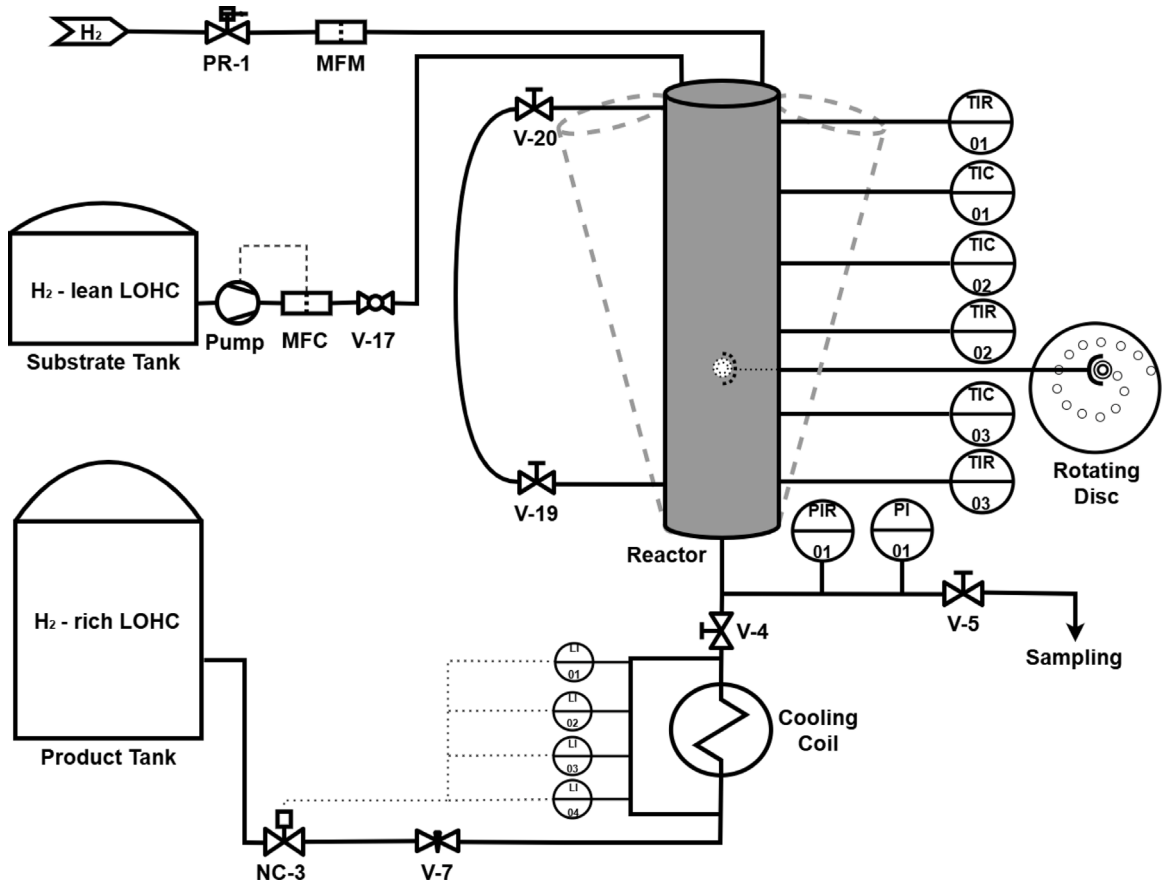

Fig. 2. Simplified plant scheme.

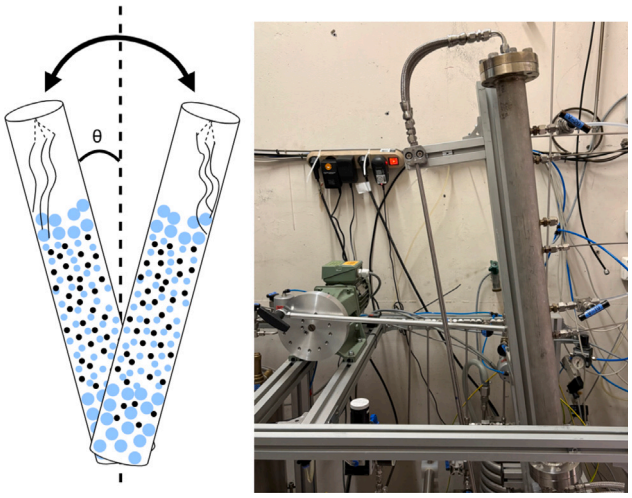

Fig. 3. Left: Sketch of reactor with glass spheres (light blue) and locally added catalysts (small black spheres) for the reactor performing oscillatory pitching motion; right: photograph of the pitching reactor for the hydrogenation experiment.

SONOCONTROL Type 1.5 SN: 10435), the NC-3 valve opened and the liquid flowed into the product tank until the liquid level in the cooling coil reached LI-3 level. This causes a sudden increase in hydrogen flow, which can be observed as spikes in Figs. 8 and 9

Table 1
Experimentally investigated catalyst packings and operation conditions.

Packing	m_{cat} (g)	CVF (vol.%)	ε_b (–)	Pressure (bar)	$\dot{m}_{HO-BT}$ (g/min)
P1	182	32	0.353	30	1
P2	60	9	0.396	20	1

CVF = catalyst volume fraction based on the total solid volume (catalyst and inert glass beads). ε_b = estimated bed void fraction. $\dot{m}_{HO-BT}$= the mass flow rate of H0-BT.

3.2. Inertization, flooding and experimental procedure

The starting of the reaction with an uneven catalyst wetting can cause insufficient use of the reactor bed and different reaction rates in different parts of the reactor. To prevent this, the same start-up procedure was applied for every experiment set [26]: As a first step, the reactor was inertisized with nitrogen by flushing the reactor 5 times with 30 bar pressure. V-19 and V-20 were opened and the reactor was subsequently flooded with benzyltoluene (H0-BT) until the catalyst filling level. The level of H0-BT was controlled from a transparent sight tube placed between V-19 and V-20. Once the H0-BT reached the catalyst level, the reactor remained flooded for 15 min to ensure proper wetting and stabilization. Subsequently, the H0-BT was completely discharged and the remaining H0-BT in the reactor bed was hydrogenated for 1.5 days by gradually increasing the temperature

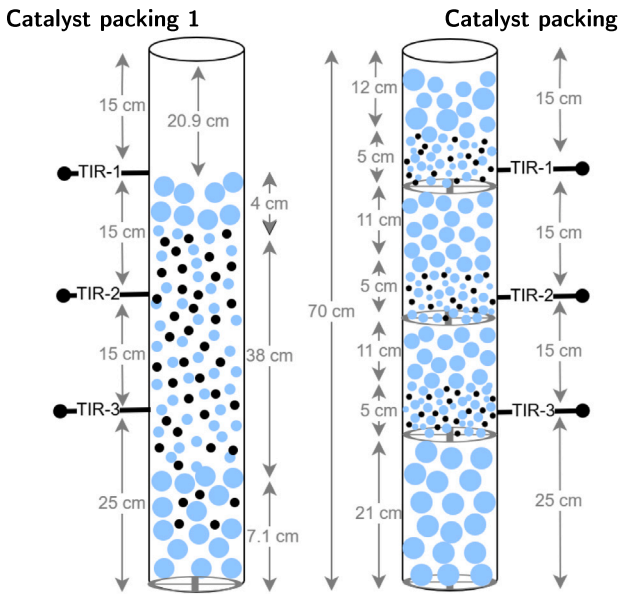

Fig. 4. Left: Sketch of catalyst packing 1; right: sketch of catalyst packing 2 with glass spheres (light blue) and locally added catalysts (small black spheres).

to 200°C and the pressure to 30 bar, and keeping it there until the hydrogen consumption decreased to 0.1 ln/min.

The plant was operated with the help of a Flexlab software. After the initialization and flooding procedure, experiments were started by increasing the temperature and pressure to the desired points. After being sure that the temperature and pressure values were constant, the reaction was started with turning on the data recording and pump for the H0-BT flow. The temperatures, pressure, hydrogen consumption and mass flow rate were followed with real-time visualization. After every flooding operation, experiments were run by changing only one parameter.

3.3. Degree of Hydrogenation (DoH) calculation

The degree of hydrogenation indicates the extent of the reaction and was calculated from MFM and gas chromatography (GC) data. Calculation from MFM data as the ratio of actual hydrogen consumption to theoretical hydrogen consumption is stated in Eq. (1), where $\dot{v}H_2$ denotes the volumetric flow rate of hydrogen, $\dot{m}_{\text{HO-BT}}$ the mass flow rate of H0-BT, $M_{\text{HO-BT}}$ the molar mass of H0-BT, R the universal gas constant, T the temperature, and p the pressure.

$$\mathbf{DoH}_{\text{MFM}} = \frac{\dot{v}H_2}{6 \times \frac{\dot{m}_{\text{HO-BT}}}{M_{\text{HO-BT}}} \times R \times \frac{T}{p}} \tag{1}$$

GC analysis was performed using Shimadzu, Model GC-2010 Plus with the Restek column (Type Rxi-17Sil MS, 30 m×0.25 mm ID, 0.25 µm film thickness) and a flame ionization detector (FID). The samples to be measured on GC were taken directly from the reactor using valve-5 (V-5). The collected samples were diluted with acetone in a 1:120 ratio in a 1.5 mL GC vial. For evaluation of the GC data, OpenChrom software was used. The degree of hydrogenation was calculated from the GC results according to Eq. (2), where $n_{H_{2,i}}$ denotes the number of hydrogen atoms bound to the component i, $n_{H_{2,\max}}$ the maximum number of hydrogen atoms that the LOHC system can bind, and x_i the mole fraction of LOHC species i. With the assumption of comparable response factors for the different hydrogenation states [27], mole fractions were calculated from the GC peak areas.

$$\mathbf{DoH} = \sum_i \frac{n_{H_{2,i}}}{n_{H_{2,\max}}} \cdot x_i$$
$$\mathbf{DoH} = \frac{A_{\text{H12-BT}} + 0.5A_{\text{H6-BT}}}{A_{\text{H12-VBT}} + A_{\text{H6-BT}} + A_{\text{H0-BT}}} \tag{2}$$

4. Simulation setup

The goal of the CFD simulations was to model the flow of the LOHC inside the reactor, in particular the liquid channeling and the influence of motion on it. For this, direct simulations were performed resolving all three phases, i.e. gaseous hydrogen, liquid LOHC and solid catalyst.

The governing equations were the conservation equations for mass, momentum and volume fraction:

$$\frac{\mathrm{d}}{\mathrm{d}t}\int_V \rho \,\mathrm{d}V + \int_S \rho(\mathbf{v}-\mathbf{v}_g)\cdot\mathbf{n}\,\mathrm{d}S = 0 \quad , \tag{3}$$

$$\frac{\mathrm{d}}{\mathrm{d}t}\int_V \rho\mathbf{v}\,\mathrm{d}V + \int_S \rho\mathbf{v}(\mathbf{v}-\mathbf{v}_g)\cdot\mathbf{n}\,\mathrm{d}S = \int_S \left(-\left(p+\frac{2}{3}\mu\nabla\cdot\mathbf{v}\right)\mathbf{I} + \mu\left(\nabla\mathbf{v}+(\nabla\mathbf{v})^{\mathrm{T}}\right)\right)\cdot\mathbf{n}\,\mathrm{d}S + \int_V \rho(\mathbf{g}+\mathbf{q})\,\mathrm{d}V \quad , \tag{4}$$

$$\frac{\mathrm{d}}{\mathrm{d}t}\int_V \alpha \,\mathrm{d}V + \int_S \alpha(\mathbf{v}-\mathbf{v}_g)\cdot\mathbf{n}\,\mathrm{d}S = 0 \quad , \tag{5}$$

with control volume V bounded by the closed surface S, velocity vector $\mathbf{v} = (u, v, w)^{\mathrm{T}}$ of the fluid, grid velocity $\mathbf{v}_g$, unit vector $\mathbf{n}$ normal to S and pointing outwards, time t, pressure p, fluid density ρ, dynamic viscosity μ, unit tensor $\mathbf{I}$, gravitational acceleration vector $\mathbf{g} = (0, 0, -9.81\,\mathrm{m/s^2})^{\mathrm{T}}$ and volume fraction α of the liquid phase, where $\alpha = 1$ (0) denotes a cell completely filled with liquid (gas). Mathematical notation follows [28]. The chemical reactions were not modeled and the flow was assumed to be incompressible and laminar. Surface tension was modeled via source term $\mathbf{q} = \omega\kappa\mathbf{n} = -\omega\nabla\cdot\left(\frac{\nabla\alpha}{|\nabla\alpha|}\right)\nabla\alpha$ as given in [29] with Kistler correlation based on [30] using default coefficients for static contact-angle modeling.

As direct simulation of the whole reactor would require an excessive computational effort, a simplified test case was studied (cf. Fig. 5): The computational domain was box-shaped with dimensions $-0.013\,\mathrm{m} \le x \le 0.013\,\mathrm{m}$, $-0.003\,\mathrm{m} \le y \le 0.003\,\mathrm{m}$ and $0\,\mathrm{m} \le z \le 0.047\,\mathrm{m}$, except that in the center of the top boundary ($z = 0.0465\,\mathrm{m}$), a cylinder with outer diameter of 0.0014 m and inner diameter of 0.001 m extended a distance of 0.006 m (inner part 0.005 m) downwards, to model the pipette from which the liquid drops down. The boundaries were set to symmetry planes, except the bottom boundary ($z = 0\,\mathrm{m}$), where the pressure outlet was located to allow fluid to leave the domain, as well as the sphere boundaries and the top boundary, which were no-slip walls, except within the top boundary for $\sqrt{x^2+y^2} \le 0.5 \times 10^{-3}\,\mathrm{m}$ on the cylinder bottom surface, where the velocity inlet was located to model the pipette's opening.

A difference compared to the real reactor was that the spheres in the numerical model did not touch each other, but were separated by an average gap of approximately $0.2D$. This gap served several purposes. First, it facilitated numerical grid generation by avoiding poor-quality cells. Such cells may occur when surfaces touch or intersect, and can result in numerical stability problems (cf. [31]). Second, the applied gap was considered a more physically correct representation of the flow in the real reactor, as there is no vertical plane in a 3D-packed catalyst-bed where the catalysts are in a perfect arrangement with no gaps in between. An average distance between catalyst spheres of $0.2D$ was selected as a reasonable match to the corresponding distances that were observed when cutting planes through the 3D packed reactor. Finally, additional simulations with smaller gaps, including the limiting case of

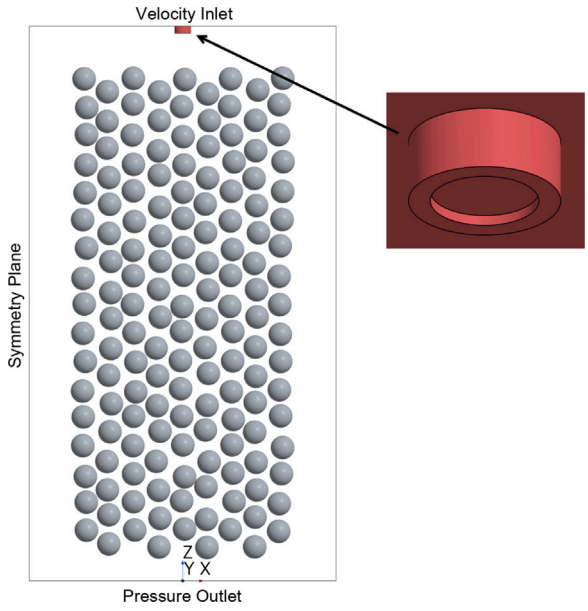

Fig. 5. Simplified reactor geometry with arbitrarily shifted catalyst spheres and zoom to pipette opening ('Velocity Inlet'), out of which liquid LOHC drops.

touching spheres, showed no significant changes in the predicted flow physics, indicating that the chosen gap does not influence the main conclusions of the study.

To generate liquid drops at a frequency of $f = 20\,\mathrm{Hz}$ with a volume $V = 0.003\,\mathrm{l}$, values for velocity $\mathbf{v}_{\mathrm{inlet}}$ and volume fraction α_{inlet} were prescribed at the inlet as

$$\mathbf{v}_{\mathrm{inlet}}(t) = \begin{cases} 0.45\,\mathrm{m/s} & \text{if } t \bmod 0.05\,\mathrm{m/s} \in [0, 0.0085\,\mathrm{s}] \\ 0 & \text{else} \end{cases}, \tag{6}$$

$$\alpha_{\mathrm{inlet}}(t) = \begin{cases} 1 & \text{if } t \bmod 0.05\,\mathrm{m/s} \in [0, 0.0085\,\mathrm{s}] \\ 0 & \text{else} \end{cases}, \tag{7}$$

where mod denotes the modulo operator.

The liquid dropped from the pipette onto the catalyst, simplified here as smooth spheres with diameter $D = 0.002\,\mathrm{m}$, to match to the average sphere size in the real reactor. On the surface of the spheres, a no-slip boundary condition was applied. The present simulations have been repeated with different contact angles, including vanishing contact angle ($\theta = 10°$, representing the experiment with reaction) and large angle ($\theta = 60°$, representing the cold-flow experiments); for space reasons, not all results are reported in detail, but the channeling behavior and break-up by motion was observed in all cases. Shown are the results for contact angles of $\theta = 10°$ and $\theta = 30°$.

As shown in Fig. 5, the reactor geometry was simplified to a catalysts arranged in a 2D plane, i.e. all sphere centers were located at $y = 0\,\mathrm{m}$. By simplifying the packing into a grid of spheres on a single plane, the number of grid cells could be reduced from an order of magnitude of 10^8 to 10^6, thus decreasing the computational cost significantly. Two configurations were studied:

- *Uniform packing*, i.e. all spheres had the same distance to their closest neighbors.
- *Randomized shifted packing*, where starting from a uniform packing with a small gap of $0.4{\times}10^{-3}$ m between spheres, every sphere was shifted randomly in the xz-plane by a distance up to 0.2×10^{-3} m to both x- and z-directions.

The first configuration is idealized and unrealistic, the second configuration is a more realistic model of the real reactor.

At initial time $t = 0\,\mathrm{s}$, the computational domain was only filled with the gas phase at zero velocity. The simulations were continued until $t_{\mathrm{sim}} = 30\,\mathrm{s}$, which corresponds to the release of 600 drops.

The flow simulations were performed using the commercial software Simcenter STAR-CCM+ version 19.06.009, which is based on the finite volume method (FVM). In order to resolve the different phases - liquid LOHC and gaseous hydrogen - the Volume of Fluid (VOF) [32] method was used with High-Resolution Interface Capturing (HRIC) [33] method to obtain a sharp interface between gas and liquid phase. In the VOF method, simulations are performed for an 'effective fluid', i.e. fluid parameters like density ρ and dynamic viscosity μ are averaged over all fluids contained in a cell, e.g. via

$$\rho = \rho_{\mathrm{liquid}}\alpha + \rho_{\mathrm{gas}}(1-\alpha) \quad , \tag{8}$$

with densities ρ_{liquid} and ρ_{gas} of the liquid and the gas phase, here $\rho_{\mathrm{liquid}} = \rho_{\mathrm{LOHC}}(T = 200°\,\mathrm{C}) = 847.92\,\mathrm{kg/m^3}$ and $\rho_{\mathrm{gas}} = \rho_{\mathrm{hydrogen}} = 0.08237\,\mathrm{kg/m^3}$.

The linearized equation system was solved by the iterative STAR-CCM+ implicit unsteady segregated solver, using an algebraic multigrid method with Gauss–Seidel relaxation scheme, V-cycles for pressure and volume fraction of water, and flexible cycles for velocity calculation. The under-relaxation factor was 0.9 for velocities, 0.95 for volume fraction and 0.3 for pressure. Per time step, a maximum of 6 iterations were performed. One iteration consisted of solving the governing equations for the velocity components, the pressure-correction equation (using the SIMPLE method for collocated grids to obtain the pressure values and to correct the velocities) and the transport equation for the volume fraction of water.

Fig. 6 shows the polyhedral grid used to discretize the domain, with local mesh refinement near all positions of interest where liquid may flow. A prism-layer mesh extended from the sphere surface, with a thickness of $0.075D$, a stretching factor of 1.5 for each successive layer and 6 layers in total. The base cell-size was $\Delta x = 1.5$ mm, which was refined by factor 0.1 near inlet and sphere surfaces. The grid consisted of $1.1 \cdot 10^6$ cells. The implicit unsteady solver was used with a constant time-step size of $\Delta t = 8 \times 10^{-5}\,\mathrm{s}$, corresponding to 625 time steps per time interval from one drop release to the next. This setup was found to produce a suitable compromise between computational efficiency and accuracy of the results. For more details, a discretization-dependence study can be found in Appendix B.

The simulations were performed in parallel on 64 CPU cores using AMD Epyc 9354 processors. With this setup, a single simulation required roughly 78 h to complete.

For details on the numerical methods, the reader is referred to standard textbooks [34].

5. Experimental results

5.1. Memory effect

Throughout the experiments, it was observed that the DoH depended not only on the process conditions, such as temperature, pressure and H0-BT flow rate, but also on experimental history. This *memory effect* was explained by channeling, which mainly results from the catalyst bed geometry. Fig. 7 shows a pronounced channeling behavior.

The influence of the memory effect was clearly observed during the experiments with the vertical and oscillatory pitching reactor. Fig. 8 shows that, compared to the vertical reactor, both hydrogen consumption rate and DoH values were larger for the oscillatory pitching reactor and for the vertical reactor after 3.5 h of oscillatory pitching motion.

The experiment with vertical reactor (Fig. 8, dash-dotted orange curve) and catalyst packing P1 at 175°C, 30 bar and 1 g/min of H0-BT flow rate was carried out after the reactor was flooded and the remaining H0-BT was hydrogenated. After 4 h of reaction, the DoH was calculated to be 78%. The vertical peaks in the graph represent

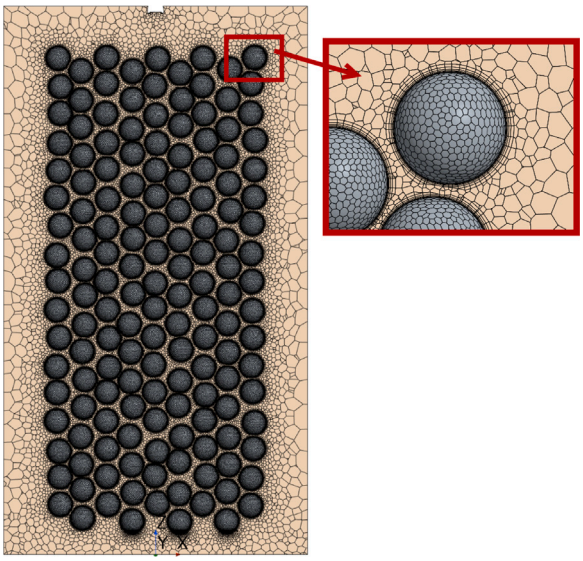

Fig. 6. Computational grid for the CFD simulations with randomized-shifted packing (left) and close-up (right) showing the prism-layers and local mesh refinement around the spheres.

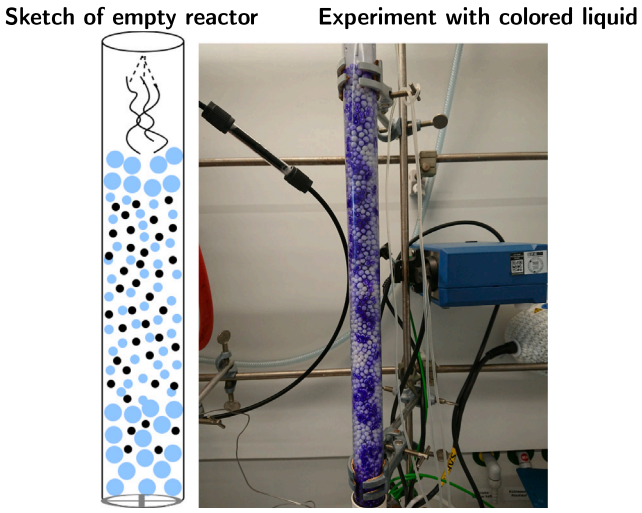

Fig. 7. Left: Sketch of reactor with glass spheres (light blue) and locally added catalysts (small black spheres) for a typical stationary reactor (no motion); right: photograph from a cold-flow experiment with colored liquid, showing the channeling in the reactor.

withdrawal of the liquid from the reservoir ('cooling coil', Fig. 2). For example, for the vertical reactor (orange curve), after the first liquid withdrawal (at ca. 1 h), the DoH-value changed drastically (from ca. 20% before to ca. 60% after withdrawal). We assume that the withdrawal disturbed the channeling and liquid distribution in the reactor. After the second withdrawal (at ca. 2.3 h), a quasi-steady state was reached, i.e. similar DoH-values were maintained after all following liquid withdrawals.

Following the vertical reactor experiment, an experiment with an oscillatory pitching reactor was run with the same operating conditions (Fig. 8, dotted green curve). Upon 2 h of oscillatory pitching motion, a DoH value of 100% was obtained.

The next day, an experiment with non-moving vertical reactor was carried out (Fig. 8, continuous blue curve) under otherwise same operating conditions and a DoH value of 100% was achieved within 1 h. The difference in vertical reactor experiments, which were carried out under the same reaction conditions but with a different experimental history, can be explained by the *memory effect*, i.e. by the breaking-up of liquid channels due to the oscillatory pitching motion. This resulted in a larger wetted catalyst surface area, which in turn enhanced the catalytic reaction. Moreover, the liquid film at the catalyst surface was renewed and disrupted by the oscillatory pitch motion, thus increasing the hydrogen availability of the active sites of the catalyst [35]. Therefore, the higher reaction efficiency continued when the reaction conditions changed from an oscillatory pitching reactor to a vertical reactor.

5.2. Effect of oscillation amplitude

Vertical reactor and oscillatory pitching reactor experiments were carried out with catalyst packing P1 and catalyst packing P2. Fig. 9 compares the hydrogen consumption and DoH values for two different catalyst packings under identical conditions (170°C, 20 bar, 1 g/min H0-BT flow rate) in a vertical reactor. As expected, DoH decreased with decreasing catalyst volume fraction as a result of the reduced number of catalyst active sites available for the reaction. However, this enabled a better understanding of the results under different experimental conditions, such as different oscillation amplitudes.

Experiments with oscillation amplitudes ±1°, ±3° and ±4° were carried out at 175°C, 30 bar, 1 g/min H0-BT flow rate and 5 s oscillating swing period (T), respectively, after the flooding process. Fig. 10 shows that increasing the oscillation amplitude from ±1° to ±3° resulted in a 36% increase in DoH, while a further increase from ±3° to ±4° led to only a 7% increase. Larger oscillation amplitudes with period T = 5 s promote improved H0-BT redistribution in the catalyst bed, resulting in effective use of the catalyst surface and reduced mass transfer limitations. This conclusion is supported by the simulation results in Appendix A.

5.3. Reproducibility of the experiments

Fig. 11 quantifies the reproducibility of the results, when repeating the experiments under identical operating conditions (175 °C, 30 bar, 1 g/min of H0-BT flow rate and with catalyst packing 1):

- Experiments with the vertical reactor (VR) starting after initial flooding of the reactor were performed twice, with a time interval of two weeks in-between, resulting in a degree of hydrogenation (DoH) of 70% and 78%.
- The experiment with the oscillatory pitching reactor (OPR) starting after initial flooding of the reactor was performed once, resulting in a DoH of 100%.
- Experiments with the OPR after VR were performed twice, with a time interval of on week in-between, resulting in a DoH of 70% (VR) followed by 91% (OPR) and 78% (VR) followed by 100% (OPR) when the VR was initially flooded, and 98% (VR) followed by 98% (OPR) when the VR was started after an additional previous OPR.
- Experiments with the VR after OPR were performed two times, with a time interval of one week in-between, resulting in a DoH of 100% (0PR) followed by 98% (VR), and 100% (OPR) followed by 100% (VR).

Fig. 11 shows averaged DoH with error bars and standard deviations. Due to the time intensive nature of the experiments, the number of repetitions was limited. However, the standard deviations are low. The observed trend is consistent across the conducted experiments and the results from 'VR after OPR' indicate the presence of a memory effect.

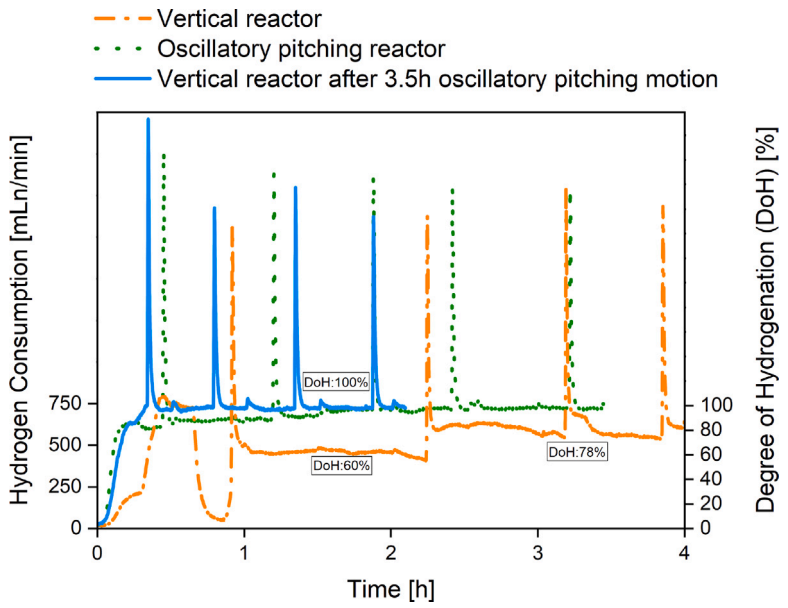

Fig. 8. Comparison of the instantaneous values for hydrogen consumption and the degree of hydrogenation (DoH) as a function of time, for the vertical non-moving reactor, for the oscillatory pitching reactor with amplitude 2.5° and period 5 s, and for the vertical non-moving reactor started after 3.5 h prior oscillatory pitching motion; with catalyst packing P1.

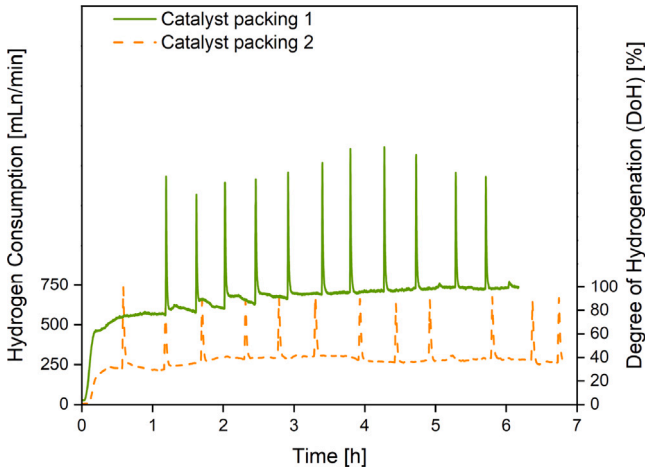

Fig. 9. Comparison of the hydrogen consumption and degree of hydrogenation results of two different catalyst packings (P1 and P2) at 170°C, 20 bar, 1 g/min H0-BT flow rate and in a vertical non-moving reactor.

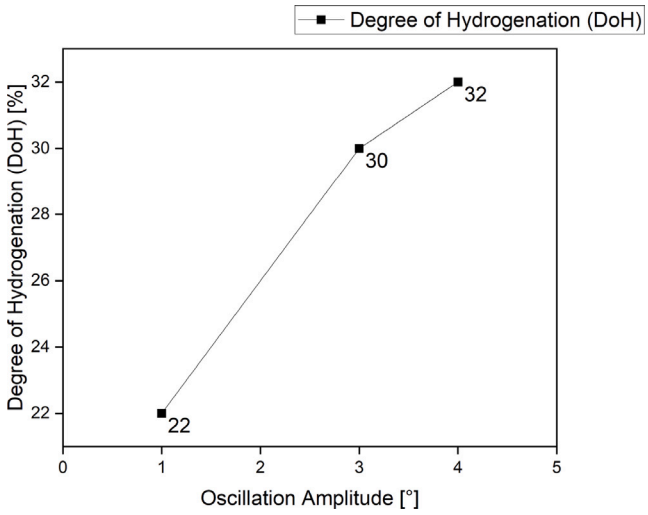

Fig. 10. Several-hour average values for degree of hydrogenation as a function of oscillation amplitude a; for reactor performing harmonic pitching motion with period $T = 5$ s, at initialized temperature $\theta = 170°$, pressure 20 bar above atmospheric pressure, mass-flow rate $\dot{m} = 1$ g/min of benzyltoluene for catalyst packing P2 (less amount of catalyst than in Fig. 8).

6. Simulation results

This section investigates whether liquid channeling, which was observed in the cold-flow experiments at room temperature with larger sphere diameter $D = 6$ mm (Fig. 7), can also be expected to occur in the real reactor (at 200° C with catalyst spheres of diameter $D = 2$ mm). This was investigated via flow simulations based on the setup described in Section 4.

For *uniform packing*, Fig. 12 shows that *no channeling occurred*. Although the liquid drops only fall onto the top center sphere, already after a comparatively short time ($t = 6$ s) all spheres were wetted, and apart from a few rows in the top and at the bottom of the packing, the wetting was spatially homogeneous, i.e. did not vary significantly with x- and z-coordinate. However, this case is rather unrealistic, as typically there is no vertical plane in the real catalyst packing where all the catalysts are uniformly spaced. Furthermore, realizing such a packing in a practical setting appears challenging.

For *randomized shifted packing*, however, Fig. 13 shows that *strong channeling occurred* in a similar manner as observed in the cold-flow experiments (cf. Fig. 7, right): The majority of the reactor was not wetted. The liquid flowed mainly along preferred paths: These channels did not establish right away, but took roughly 8 s, or 160 drops, for the flow to find its preferred path downwards, which then remained until the end of the simulation at $t = 30$ s.

Figs. 13 and 14 show that similar channeling occurred both with contact angle $\theta = 30°$ (resembling contact angles in the cold-flow experiments) and $\theta = 10°$ (resembling contact angles in the hot LOHC reactor). Therefore, the experimentally observed channeling in the cold-flow experiments can also be expected to occur in the hot LOHC reactor, underlining the relevance of cold-flow experiments.

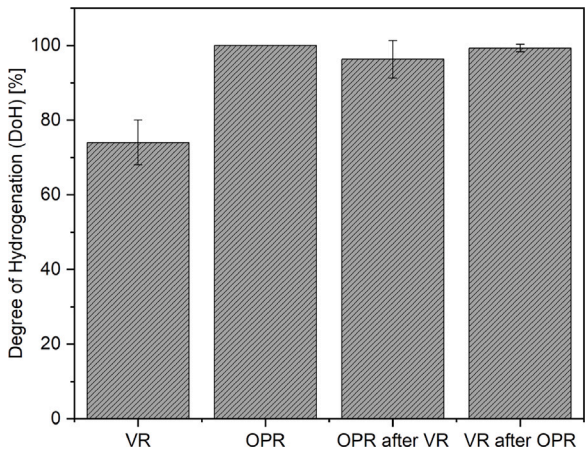

Fig. 11. Degree of hydrogenation for different reproducibility experiments at 175°C, 30 bar, 1 g/min H0-BT flow and catalyst packing P1. Here, VR and OPR represent vertical reactor and oscillatory pitching reactor, respectively. Shaded bars represent mean value for repeated experiments and error bars indicate maximum deviation ϵ between repeated experiments; the corrected sample standard deviation σ were 5.6% (VR), 4.7% (OPR after VR) and 1.2% (VR after OPR).

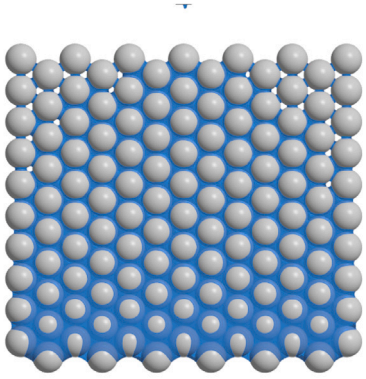

Fig. 12. Simulation results for stationary reactor (no motion) showing liquid LOHC (blue) on perfectly evenly spaced spheres, after $t = 6$ s simulation time, resulting in uniform wetting without channeling.

Fig. 15 shows how the pitching motion broke up the channeling that occurred in the non-moving reactor. For this, starting from the vertical reactor, the pitching angle θ (cf. Fig. 3) was varied as $\theta = \theta_a \sin(\omega t)$ with pitch amplitude $\theta_a = 20\,\text{deg}$, angular wave frequency $\omega = 2\pi/T$ and period $T = 3\,\text{s}$. Pitching corresponds to rotation around the y-axis, with center of rotation equal to the center of the coordinate system in Fig. 5 (bottom floor center).

Fig. 16 visualizes where liquid occurred during the last 20 s of simulated time. In the non-moving reactor (left image), substantial parts of the blue-colored areas are cut-off from the trickling flow, and hence not supplied with fresh liquid; therefore, the part of the reactor that participates in the reaction will be even smaller than the blue areas in the left image suggest. In contrast, in the moving reactor (right image), fresh liquid is resupplied to most of the blue areas, so the blue areas should correlate with the amount of reaction taking place. Results for contact angle $\theta = 30°$ looked similar and hence are not shown.

Fig. 17 shows results of flow simulations performed with a realistic 3D catalyst packing. For this, a cylindrical reactor segment with a diameter of $D \approx 0.022\,\text{m}$ and a height of $h \approx 0.046\,\text{m}$ was considered. Apart from the realistic catalyst packing, the simulation setup was identical to that used in the simplified configuration shown in Fig. 15. The simulations were carried out over a duration of 30 s for both a stationary and a moving reactor. To obtain realistic reactor motions, the motions of the 5 MW ProHyGen platform were first computed with the in-house potential-flow solver *pan*MARE. The platform was subjected to a realistic seaway, i.e. a JONSWAP spectrum with $\cos^2$ directional spreading, significant wave height $H_s = 8.45\,\text{m}$, peak wave period $T_{peak} = 13.62\,\text{s}$ and wind speed $v_{wind} = 19.6\,\text{m/s}$. The main directions of wind and wave propagation were aligned with the x-axis. The resulting motions were subsequently prescribed as the reactor motion in the present CFD simulations. Since the final location of the LOHC reactor on the floating platform had not yet been determined at the time of conducting the simulation, the rotations and motions were applied assuming that the center of gravity of the floating platform coincided with the origin of the local coordinate system shown in Fig. 17, which was located 0.003 m below the center of the cylinder bottom. Consequently, the reactor underwent six-degree-of-freedom motion, with the oscillatory surge motion (translation in the x-direction) and pitching motion (rotation about the y-axis) being the dominant motion components.

As before, liquid channeling occurred in the non-moving reactor, whereas reactor motion broke-up the channeling. The breaking-up of the channeling occurred mainly in y-direction, i.e. along the path traversed by the dominant motions. The results qualitatively agreed with the simplified setup.

Applying a few degrees of stationary inclination to the non-moving reactor (±2° around the y-axis) did not alter the liquid path substantially, nor did refining the discretization change the channel paths. This indicates that the channel paths are not coincidence, but instead determined by the geometrical packing. The path of the channeling appeared to be highly dependent on the positioning of each sphere in the packing.

Preliminary investigations of larger, constant tilting angles suggested that, although the path can differ dependent on the inclination, it can be assumed that the fluid will always find a steady path to flow down as long as factors like the inlet flow rate or inclination remains constant.

7. Discussion

The present work presented the *first experimental demonstration that applying oscillatory motion can substantially increase the reaction efficiency for hydrogenation in a trickle-bed reactor*. When oscillatory pitching motion was applied, the reaction approached steady-state efficiency much faster. The degree of hydrogenation (DoH) remained above 80% already from 10 min after the reaction was started, and then approached 100% (cf. Fig. 8). In contrast, the conventional non-moving reactor needed 14 times as long to reach a DoH of 78%, and remained mostly below this value during the rest of the 4 h of experiment.

The present results demonstrate that the reaction efficiency could be substantially altered by varying the oscillation amplitude. For the reported test-case in Fig. 10, increasing the pitching amplitude from 1° to 4° resulted in a 45% increase in hydrogenation, with a roughly linear relationship between DoH and oscillation amplitude in the investigated range. This finding implies that reactor motion could potentially become a practical technique to adjust reaction speed.

For the proposed floating platform from the ProHyGen project (cf. Section 2), the present results suggest that the natural platform motion will suffice to improve reaction efficiency as observed in Fig. 17. Thus, no active motion strategy is required: The more wind, waves and electricity are available, the larger will be the reactor motions and reaction efficiency.

The second key finding from the present hydrogenation experiments was that, if the reactor had previously been subjected to oscillatory motion, it maintained the high reaction efficiency (i.e. DoH ≈ 100%, cf. Fig. 8) for more than two hours. This demonstrates that *there is a strong memory effect related to past motions of the reactor*. Furthermore,

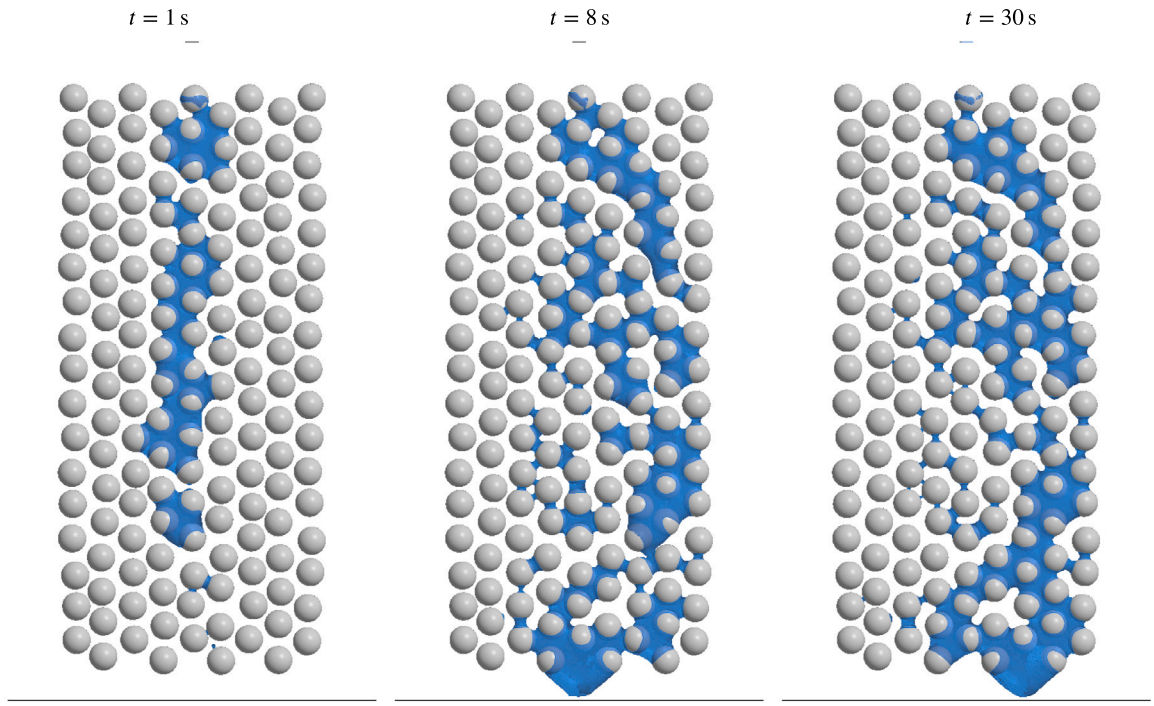

Fig. 13. Simulation results for stationary reactor (no motion) showing liquid LOHC (blue) with *contact angle* $\theta = 30°$ on spheres with slight random shifts in XZ-direction, resulting in channeling, which established not directly (left image, $t = 1$ s) but after a comparatively short time (center image, $t = 8$ s) and remained after (right image, $t = 30$ s).

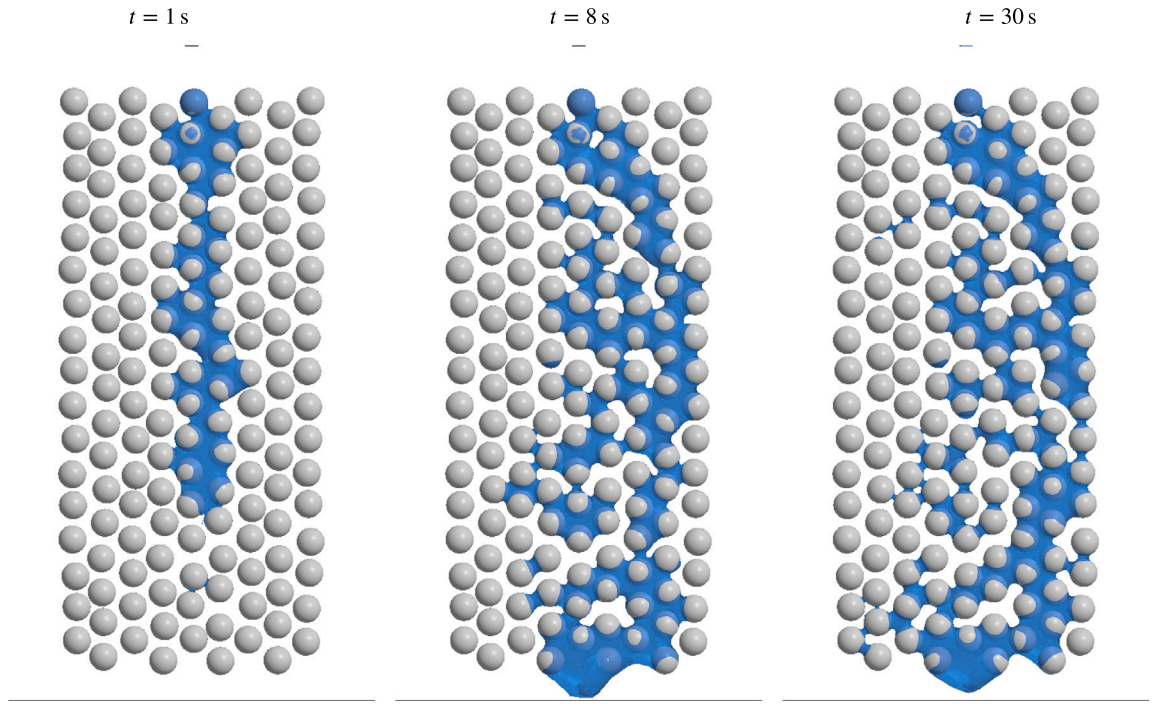

Fig. 14. As Fig. 13 for stationary reactor (no motion), except for *contact angle* $\theta = 10°$; similar channeling occurred as for the larger contact angle.

this shows that it may not be necessary to have constant oscillatory motion, but that reaction efficiency could potentially be substantially increased by only occasional application of motion to the reactor.

These experimentally observed phenomena are not yet fully understood, because at present, the details of the flow and reaction inside the reactor are not known, and cannot be determined by state-of-the-art approaches to the problem. Therefore, there is a need to develop new experimental and numerical techniques, to provide a detailed understanding of the related physics. This holds the prospect for better control of the reaction.

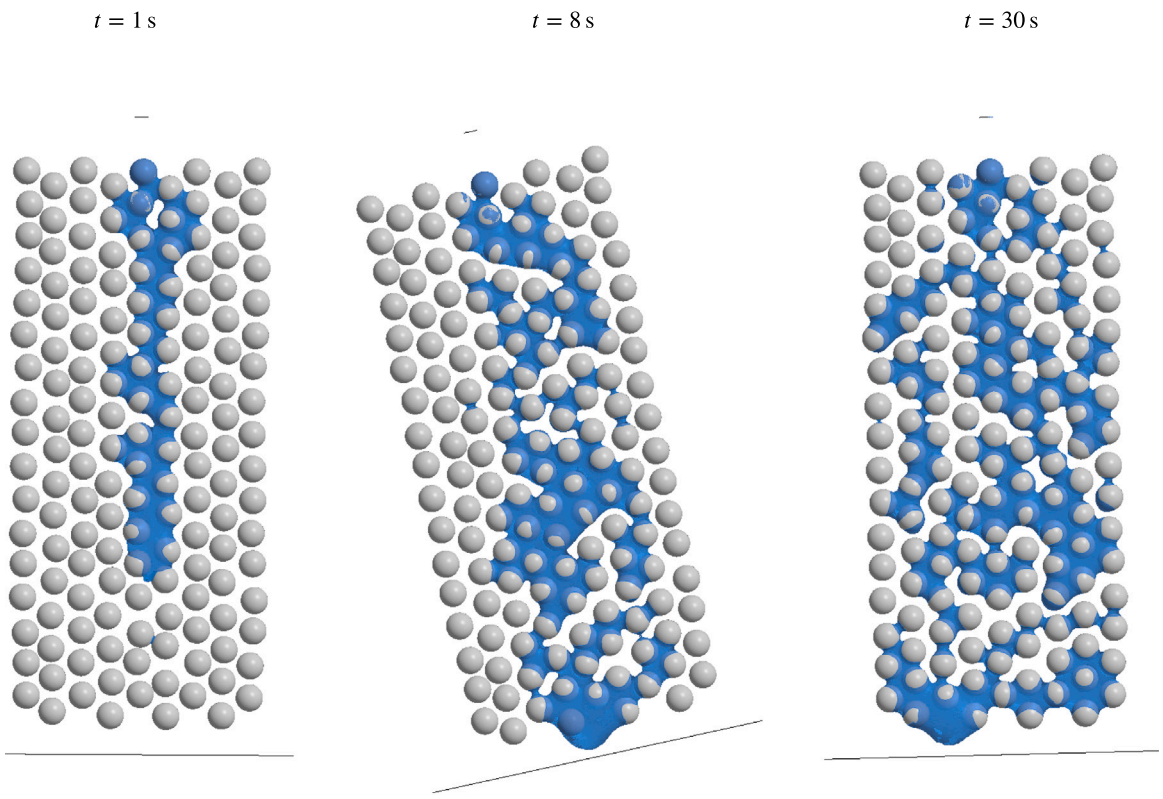

Fig. 15. As Fig. 13, except for oscillatory pitching reactor with period $T = 3$ s and amplitude $\theta_a = 20°$.

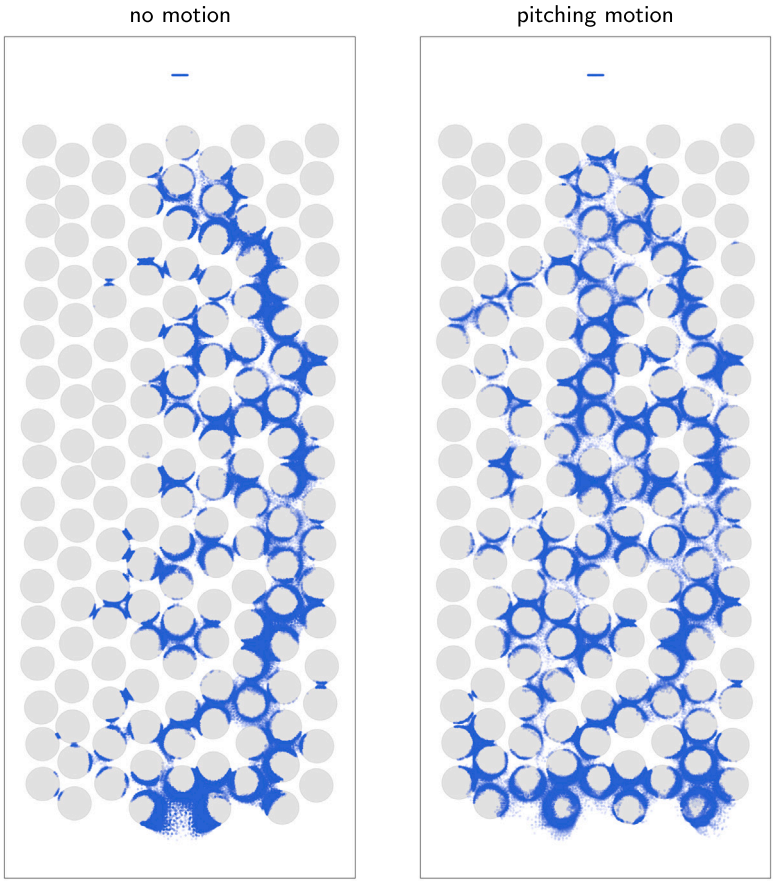

Fig. 16. Locations where liquid occurred (blue) within times $t \in [10\,\text{s}, 30\,\text{s}]$; for CFD simulations with LOHC at temperature 200 °C and contact angle $\theta = 10°$; pitching motion (right) with amplitude of 20° and period of 3 s broke-up the channeling that occurred in the not-moving reactor (left).

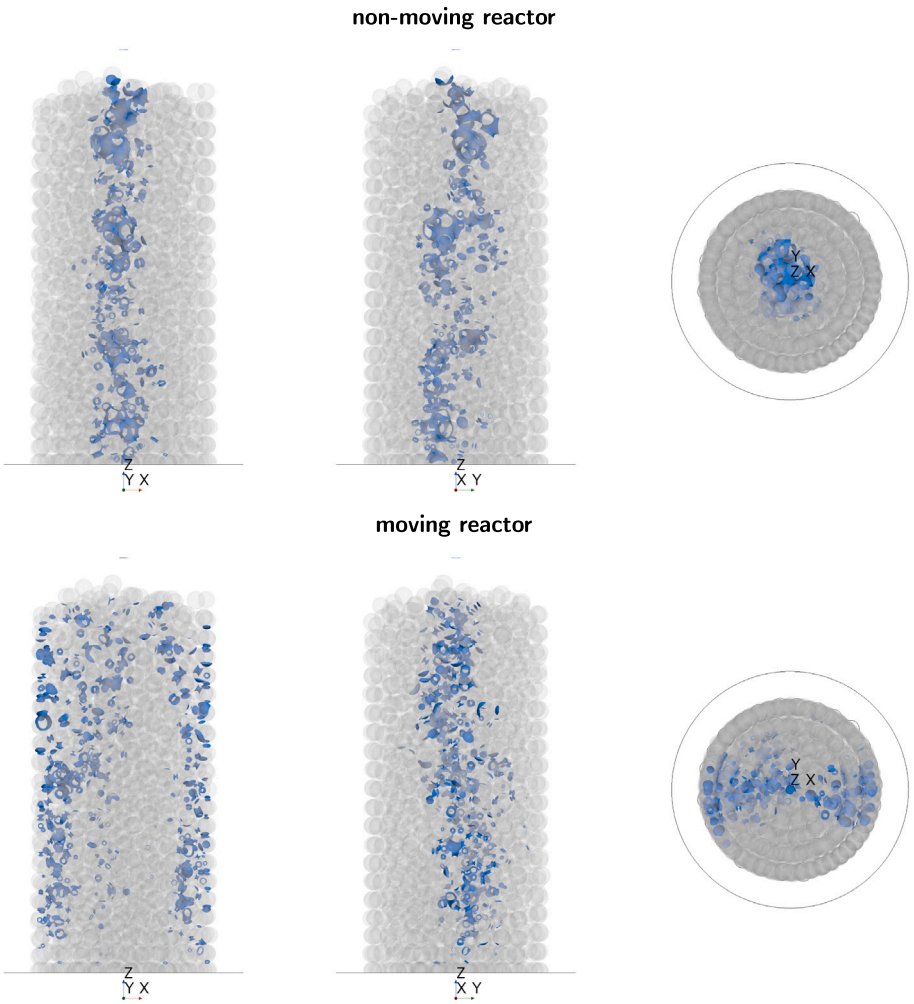

Fig. 17. As Fig. 13, except for realistic 3D-packed catalyst bed in a reactor that is non-moving (top) or moving with 6 degrees of freedom in a realistic sea state (bottom); for front view (left), side view (middle) and top view (right) in a local coordinate system moving with the reactor (shown below the packed bed) at time instant $t = 30$ s; the reactor motion broke up the channeling and increased wetting especially in x-direction (i.e. dominant motion direction).

This work provided an important first step towards a detailed understanding of the aforementioned phenomena, by proposing a theory that explains them, based on strong data from both cold-flow experiments and CFD simulations:

This *work proposed that liquid channeling is an inherent feature of trickle-bed reactors for LOHC hydrogenation, and that, by applying oscillatory motion to the reactor, these channels can be broken up, resulting in increased reaction efficiency*: This would mean that, in the non-moving reactor, the majority of the trickle-bed reactor does not take part in the chemical reaction. Instead, most of the liquid would flow along narrow channels, which are defined by the geometry of the catalyst bed. Even if wetting occurs outside these channels, there would be no supply of fresh liquid and no transport of old liquid, which implies that the liquid in these parts would quickly saturate and the local reaction efficiency would drop towards zero relatively quickly. Therefore, the reaction of interest would only take place in the vicinity of the liquid channels. Simulation results in Figs. 13–16 show that, by applying oscillatory pitching motion to the reactor, the channeling can be broken-up, resulting in increased wetting and supply of fresh liquid in the majority of the reactor, which consequently increases the reaction speed.

That channeling can occur in trickle-bed reactors was demonstrated by cold-flow experiments shown in Fig. 7. However, the cold-flow experiments were performed without chemical reaction, for different fluids, different temperature and different size of spheres representing the catalyst, so the question was whether such channeling would also occur in the real reactor under operating conditions.

The present *results from CFD simulations* of a simplified reactor geometry *indicate that channeling will indeed occur in the real reactor at operation*: The CFD simulations showed that, as soon as there is some irregularity in the packing of catalyst spheres, channels with similar shape as in the cold-flow experiments occurred. The simulations were performed for same temperature, same liquids and similar catalyst size as in the real reactor. Varying these parameters also resulted in comparable channeling. A discretization-dependence study was performed to show that the behavior remains when discretization errors are reduced (cf. Appendix B). Although the final experimental proof is missing, the evidence is already strong that the proposed theory adequately explains the unexpected phenomena observed in the hydrogenation experiments.

Based on the present results, the following *physical mechanism behind the aforementioned memory effects is proposed*. A possible explanation is that the liquid channeling, i.e. the preferred flow paths within the reactor, is determined (at least partly) by the geometry of the catalyst bed. Next, assume that there will be various parts along the liquid channels, where the liquid could continue into different directions, i.e. the geometry does not impose a strong preference for a single direction. If at these locations there is already an established channel, then effects like surface tension could dictate the flow direction. Thus, an existing channel would have an intrinsic stability, and would require reactor motion exceeding a certain threshold to be broken up. Accordingly, prior reactor motion may establish a denser network of channels,

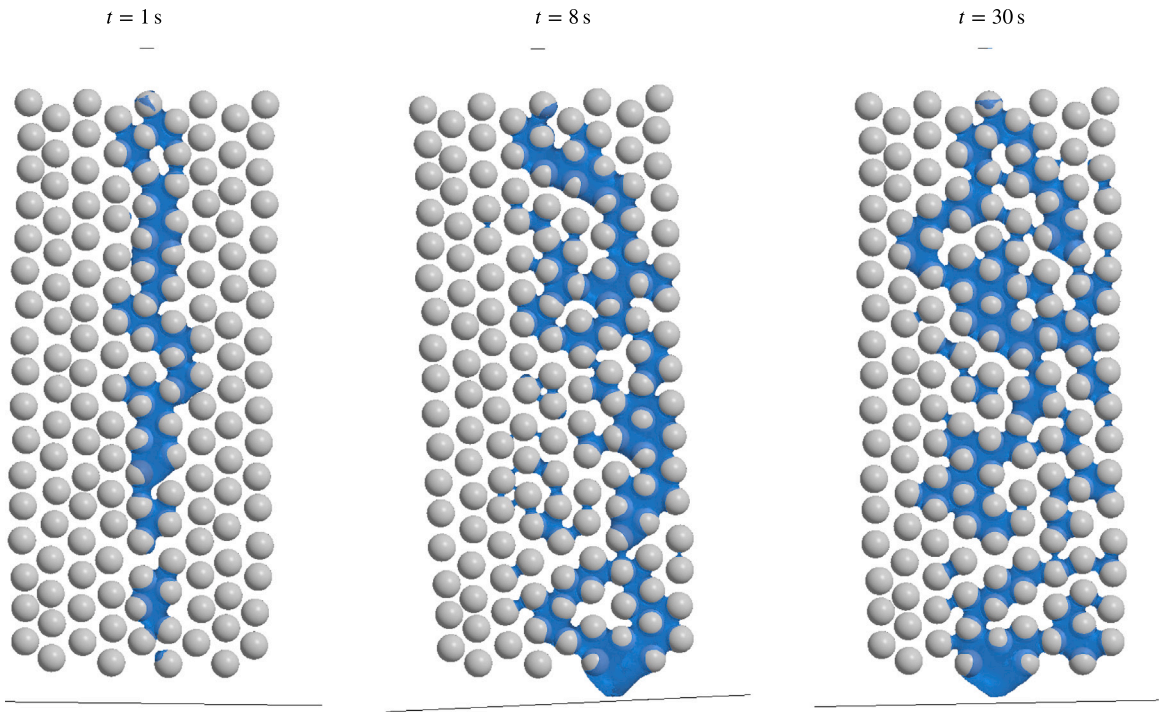

Fig. 18. As Fig. 13, except for oscillatory pitching reactor with period $T = 5$ s and amplitude $\theta_a = 4°$.

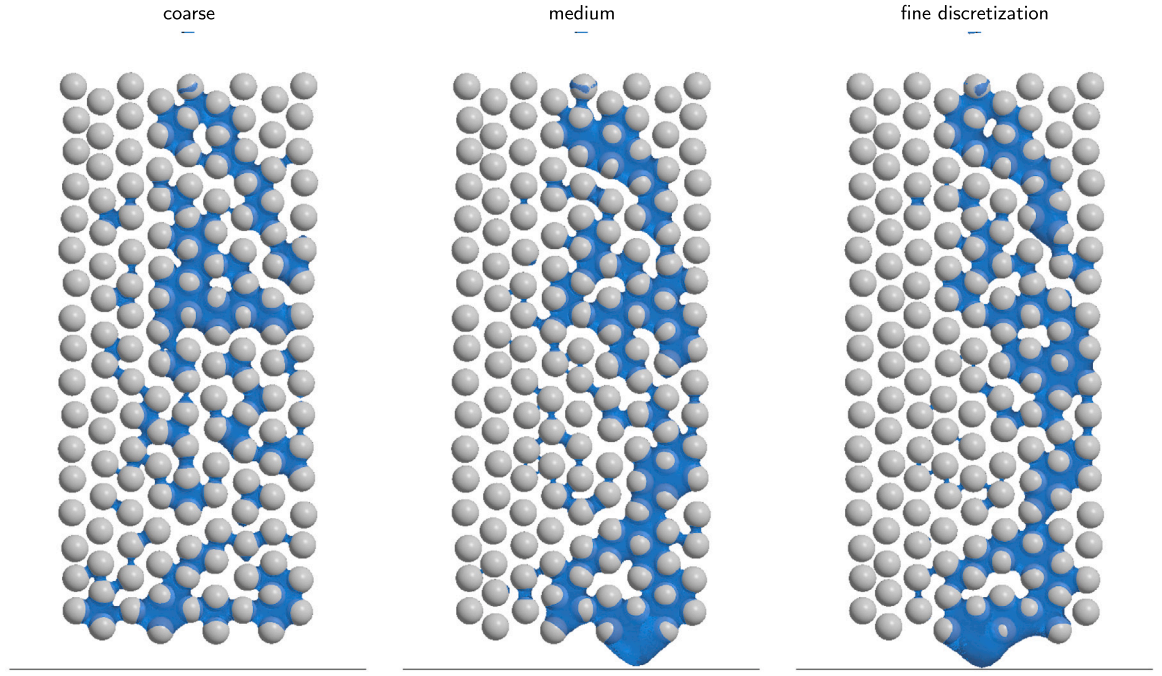

Fig. 19. As Fig. 13 at time $t = 30$ s ('medium'), with additional results for simulations repeated with factor $\sqrt{2}$ ($\frac{1}{\sqrt{2}}$) coarser (finer) grid and time-step.

that may persist for surprisingly long times after the reactor motion is stopped. This would explain the observed increase in reaction efficiency for the non-moving reactor, if it had performed prior oscillatory motion (blue curve in Fig. 8).

The good agreement between the proposed simplified test case (Figs. 13–16) and the 3D-packed reactor (Fig. 17) indicates that *the simplified test-case is capable of predicting breaking-up of channeling* in the 3D reactor, at much lower computational effort. Furthermore, the simplified configuration is well suited for experimental investigations of the underlying fluid dynamics. Therefore, the proposed simplified test-case provides a practical framework for studying a wide range of trickle-bed reactors and for systematically investigating the influence of key parameters, including reactor motion as well as catalyst size and geometry, on the internal flow behavior. As a side-note, the simulation results also indicate that reaction efficiency could be substantially increased, if a sufficiently uniform packing of the catalyst were realized (cf. Fig. 12). An interesting topic for future study would be to investigate how large irregularities can become before the wetting ceases to be spatially homogeneous. The outcome of such investigations could

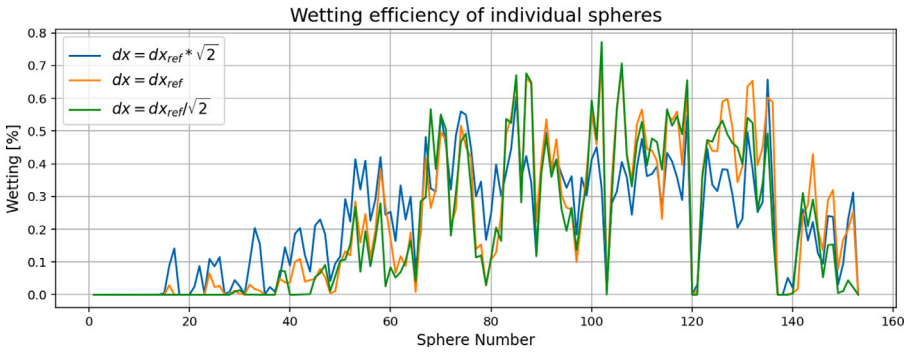

Fig. 20. Average wetting of individual spheres within the times $t \in [20, 30]$ s, for the simulations from Fig. 19 with coarse ($dx = dx_{ref} * \sqrt{2}$), medium ($dx = dx_{ref}$) and fine ($dx = dx_{ref}/\sqrt{2}$) discretization; with sphere numbering as seen in Fig. 20; the liquid channeling is shown by the highly non-uniform wetting; close agreement between regions of low (high) wetting, esp. between medium and fine discretization, sufficient convergence towards a discretization-independent solution.

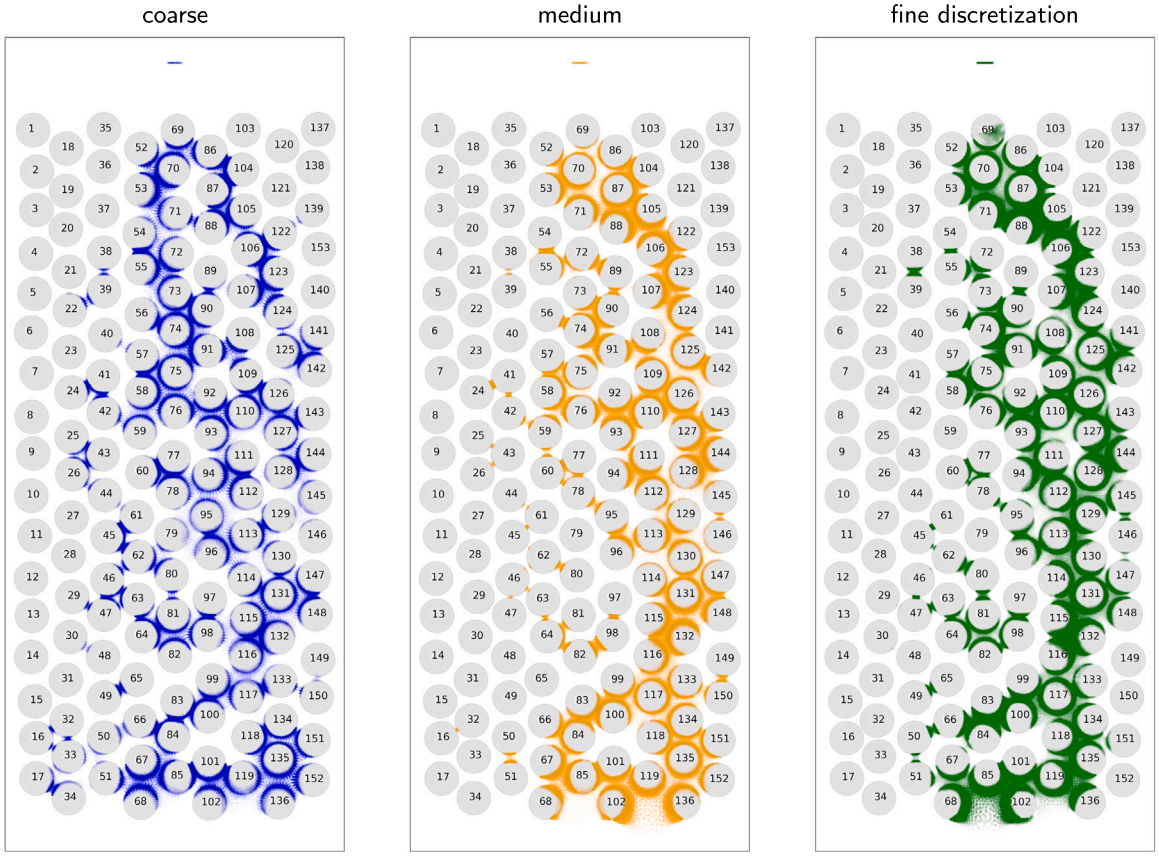

Fig. 21. Locations where liquid occurred (colored blue, orange or green) within the times $t \in [20, 30]$ s, for the simulations from Fig. 19; strong (light) color indicates frequent (rare) presence of liquid.

have important implication concerning whether such a configuration could be realized in practice.

Therefore, it is anticipated that the present findings will be applicable to many other types of trickle-bed reactors, and open up a wide range of new research questions, including:

- Which oscillation periods and amplitudes are the most effective, energy-efficient, and economically viable for enhancing the performance of a given trickle-bed reactor?
- Which degrees of freedom of reactor motion (oscillatory translation along and/ or rotation around all three coordinate axes) are most effective at disrupting or preventing the formation of preferential liquid channels?
- How do the detailed multiphase flow, liquid distribution, and chemical reaction evolve within the reactor under oscillatory motion?
- Would non-harmonic oscillations such as they occur naturally atop floating structures in the ocean, potentially enhance channel disruption more effectively than harmonic oscillations?

At present, the optimal motion strategy for a trickle-bed reactor remains an open research question. Furthermore, the effects of motions on the other process technologies on the floating platform, like electrolysis or desalination, and their interplay with the hydrogenation reactor, remains a topic for future research, as well (cf. [36,37]).

The present findings suggest that *reactor motion could enable lower-pressure operation*: For the same settings and the same amount of

catalyst, improved wetting due to the reactor motion will enable more catalyst to take part in the reaction, thereby lowering the pressure demand to reach same hydrogenation rates.

Future research should combine further development of CFD simulation techniques with new experimental techniques, to provide a deeper understanding of the flow features inside trickle-bed reactors. This holds potential to achieve higher efficiency in smaller reactors, and perhaps a means to adjust reaction speed, e.g. to adjust to time-varying availability of electricity from renewable energies. The floating offshore wind turbine concept presented in this work illustrates one example, where this capability could provide an important benefit.

Future work will extend the simulations to include chemical reactions and heat transfer. This will require the development of efficient numerical approaches capable of predicting where reactions occur within the reactor and how the local and global fluid dynamics influence reaction efficiency. Such developments have the potential to significantly improve the design and optimization of trickle-bed reactors across a wide range of industrial applications.

8. Conclusion

The present work demonstrated that applying oscillatory pitching motion can substantially increase the reaction efficiency for hydrogenation in a trickle-bed reactor: The degree of hydrogenation (DoH) remained above 80% already from 10 min after the reaction was started, which was 14 times faster than without reactor motion. With oscillatory pitching motion, DoH quickly reached nearly 100%, whereas it remained around 80% or lower without reactor motion.

An important finding for practical application was that, to obtain such an efficiency increase, the motion does not need to be applied continuously: The reported results showed strong memory effects, i.e. DoH could be maintained around 100% for 2 h in a non-moving reactor, if the reactor had been operated under oscillatory pitching motion beforehand. Therefore, substantial efficiency increases could be achieved by only occasional reactor motions.

The present results demonstrate that the reaction efficiency could be substantially altered by varying the oscillation amplitude. For the reported test-case, increasing the pitching amplitude from 1° to 4° resulted in a 45% increase in hydrogenation, with a roughly linear relationship between DoH and oscillation amplitude in the investigated range. This finding implies that reactor motion could potentially become a practical technique to adjust reaction speed. This could be beneficial for reactors operated by renewable energies, enabling reactors to adjust their reaction speed even to a strongly varying electricity supply.

This work proposes that liquid channeling is an inherent feature in trickle-bed reactors for LOHC hydrogenation, and that, by applying oscillatory motion to the reactor, these channels can be broken up, resulting in increased reaction efficiency. This theoretical explanation was supported by flow visualization in cold-flow experiments and CFD simulations that fully resolved the gas, liquid and solid phase. A final proof of this theory is subject to ongoing investigations. It requires development of new experimental and numerical techniques to understand the detailed flow and reaction dynamics within the reactor.

Topics for future research include a detailed study on how different types of reactor motion affect reaction speed in trickle-bed reactors for LOHC hydrogenation. It is anticipated that the present findings will be applicable to many other types of trickle-bed reactors as well.

CRediT authorship contribution statement

Bilge Su Subasi: Writing – review & editing, Writing – original draft, Investigation, Formal analysis, Data curation. **Triani Nur Zahra:** Writing – review & editing, Writing – original draft, Software, Investigation, Formal analysis, Data curation. **Andreas Bösmann:** Writing – review & editing, Writing – original draft, Supervision, Project administration, Funding acquisition, Conceptualization. **Robinson Perić:** Writing – review & editing, Writing – original draft, Supervision, Project administration, Conceptualization. **Peter Wasserscheid:** Writing – review & editing. **Moustafa Abdel-Maksoud:** Writing – review & editing, Supervision, Funding acquisition, Conceptualization.

Declaration of competing interest

The authors declare that they have no known competing financial interests or personal relationships that could have appeared to influence the work reported in this paper.

Acknowledgments

Funding by BMWE for the ‘Verbundvorhaben: ProHyGen - Prototypenentwicklung eines schwimmenden Offshore-H2-Generators und Planung von GW-Offshore-Wasserstoffparks; Reaktionstechnische Untersuchungen der Speichereinheit eines schwimmenden Offshore-H2-Generators’ (engl. ‘Joint Project: ProHyGen - Prototype development of a floating offshore H2 generator and planning of GW-scale offshore hydrogen parks; Reaction engineering investigations of the storage unit of a floating offshore H2 generator’), FKZ 03EI3084 is gratefully acknowledged.

Appendix A

This section investigates whether pitching amplitudes of a few degrees are sufficient to break up the liquid channeling. For this purpose, the simulation presented in Fig. 15 was repeated, using a larger period ($T = 5\,\mathrm{s}$) and a smaller pitching amplitude $\theta_a = 4\,\mathrm{deg}$. These settings were identical to those used for the rightmost experimental data point in Fig. 10 for the hot pitching reactor.

Fig. 18 shows that breaking-up of the channeling could clearly be observed in the flow simulations. However, it was less pronounced than in the case with the larger pitching amplitude of $\theta_a = 20\,\mathrm{deg}$ shown in Fig. 15. The present results therefore indicate a clear trend towards more effective breaking-up of liquid channeling with increasing pitching amplitude. This provides an explanation for the experimentally observed increase in reaction efficiency with increasing reactor motion shown in Fig. 10.

Appendix B

This section presents the results of a grid- and time-step dependence study. Since second-order spatial and temporal discretization schemes were used throughout, reducing the grid spacing and time step by a factor of $\frac{1}{\sqrt{2}}$ decreases the corresponding discretization errors by approximately a factor of $\left(\frac{1}{\sqrt{2}}\right)^2 = \frac{1}{2}$. Accordingly, the study was performed using three levels of spatial and temporal discretization, with each level refined by a factor of $\frac{1}{\sqrt{2}}$ relative to the previous one. Under these conditions, the difference between the coarse and medium discretizations is expected to be approximately twice that between the medium and fine discretizations. This behavior provides evidence of convergence towards a discretization-independent solution. The medium discretization corresponds to the setup used throughout the remainder of this work.

Figs. 19–21 show that, as expected, the differences between the coarse and medium discretizations were noticeably larger than those between the medium and fine discretizations. Furthermore, the remaining differences between the medium and fine discretizations were sufficiently small to indicate that additional refinement would not lead to

any substantial changes in the predicted flow field.[1] The results therefore demonstrate convergence towards a discretization-independent solution. Consequently, the medium discretization was selected as an appropriate compromise between computational efficiency and the accurate resolution of the underlying flow physics.

Data availability

All data supporting the findings of this publication are openly available in Zenodo at https://doi.org/10.5281/zenodo.19662048. In particular, videos of the figures showing CFD simulation results are available under this link.

References

[1] C.N. Satterfield, Trickle-bed reactors, AIChE J. 21 (2) (1975) 209–228, http://dx.doi.org/10.1002/aic.690210202.

[2] J. Tan, Y.-N. Ji, W.-S. Deng, Y.-F. Su, Process intensification in gas/liquid/solid reaction in trickle bed reactors: A review, Pet. Sci. 18 (4) (2021) 1203–1218, http://dx.doi.org/10.1016/j.petsci.2021.07.007.

[3] P.M. Modisha, C.N.M. Ouma, R. Garidzirai, P. Wasserscheid, D. Bessarabov, The prospect of hydrogen storage using liquid organic hydrogen carriers, Energy Fuels 33 (4) (2019) 2778–2796, http://dx.doi.org/10.1021/acs.energyfuels.9b00296.

[4] F.S. Mederos, J. Ancheyta, J. Chen, Review on criteria to ensure ideal behaviors in trickle-bed reactors, Appl. Catal. A: Gen. 355 (1) (2009) 1–19, http://dx.doi.org/10.1016/j.apcata.2008.11.018.

[5] A. Azarpour, N. Rezaei, S. Zendehboudi, Performance analysis and modeling of catalytic trickle-bed reactors: a comprehensive review, J. Ind. Eng. Chem. 103 (2021) 1–41, http://dx.doi.org/10.1016/j.jiec.2021.04.020.

[6] I. Stamatiou, F.L. Muller, Determination of mass transfer resistances in trickle bed reactors, Chem. Eng. J. 377 (2019) 119808, http://dx.doi.org/10.1016/j.cej.2018.08.194.

[7] Y. Tang, G. Luo, J. Zhong, K. Chen, C. Xu, Z. Cheng, Effects of stagnant zone on the effectiveness factor in a trickle bed, Chem. Eng. Sci. 248 (2022) 117211, http://dx.doi.org/10.1016/j.ces.2021.117211.

[8] L. Baussaron, C. Julcour-Lebigue, A. Wilhelm, H. Delmas, C. Boyer, Wetting topology in trickle bed reactors, AIChE J. 53 (7) (2007) 1850–1860, http://dx.doi.org/10.1002/aic.11189.

[9] H. Deng, B. Guo, H. Dong, C. Liu, Z. Geng, Computational investigation of liquid holdup and wetting efficiency inside trickle bed reactors with different catalyst particle shapes, Appl. Sci. 10 (4) (2020) 1436, http://dx.doi.org/10.3390/app10041436.

[10] L. Baussaron, C. Julcour-Lebigue, A.-M. Wilhelm, C. Boyer, H. Delmas, Partial wetting in trickle bed reactors: measurement techniques and global wetting efficiency, Ind. Eng. Chem. Res. 46 (25) (2007) 8397–8405, http://dx.doi.org/10.1021/ie070030b.

[11] J. Geiling, L. Wagner, F. Auer, F. Ortner, A. Nuß, R. Seyfried, F. Stammberger, M. Steinberger, A. Bösmann, R. Öchsner, P. Wasserscheid, K. Graichen, M. März, P. Preuster, Operational experience with a liquid organic hydrogen carrier (lohc) system for bidirectional storage of electrical energy over 725 h, J. Energy Storage 72 (2023) 108478, http://dx.doi.org/10.1016/j.est.2023.108478.

[12] A.M. Dashliborun, Performance of multiphase packed-bed reactors and scrubbers on offshore floating platforms: hydrodynamics, chemical reaction, cfd modeling and simulation, 2018.

[13] A.M. Dashliborun, J. Zhang, S.M. Taghavi, F. Larachi, 110Th anniversary: Marinization of multiphase reactors through the prism of chemical engineers, Ind. Eng. Chem. Res. 58 (8) (2019) 2607–2630, http://dx.doi.org/10.1021/acs.iecr.8b05695.

[14] J. Zhang, Hydrodynamic Behavior of Packed-Bed Reactors on a Floating Platform : Liquid Distribution and Drainage Dynamics (Ph.D. thesis), Université Laval, Quebec, Canada, 2021.

[15] I. Iliuta, F. Larachi, Fischer–Tropsch synthesis in vertical, inclined and oscillating trickle-bed reactors for offshore floating applications, Chem. Eng. Sci. 177 (2018) 509–522, http://dx.doi.org/10.1016/j.ces.2017.12.012.

[16] I. Iliuta, F. Larachi, Hydrocarbon hydrodesulfurization in vertical, inclined and oscillating trickle beds – hydrodynamics & reactor performance for offshore petroleum marine applications, Fuel 186 (2016) 35–49, http://dx.doi.org/10.1016/j.fuel.2016.08.059.

[17] M.T. Shah, R.P. Utikar, V.K. Pareek, Effect of column inclination and oscillation on liquid spreading in a trickle bed, Chem. Eng. Res. Des. 152 (2019) 165–179, http://dx.doi.org/10.1016/j.cherd.2019.09.037.

[18] WindSeeG, Gesetz zur entwicklung und förderung der windenergie auf see. german bill on development of offshore wind energy, 2016.

[19] P. Preuster, A. Alekseev, P. Wasserscheid, Hydrogen storage technologies for future energy systems, Annu. Rev. Chem. Biomol. Eng. 8 (2017) 445–471, http://dx.doi.org/10.1146/annurev-chembioeng-060816-101334.

[20] P. Preuster, C. Papp, P. Wasserscheid, Liquid organic hydrogen carriers (lohcs): Toward a hydrogen-free hydrogen economy, Acc. Chem. Res. 50 (1) (2017) 74–85, http://dx.doi.org/10.1021/acs.accounts.6b00474, pMID: 28004916.

[21] A. Tremel, P. Wasserscheid, M. Baldauf, T. Hammer, Technoeconomic analysis for the synthesis of liquid and gaseous fuels based on hydrogen production via electrolysis, Int. J. Hydrog. Energy 40 (35) (2015) 11457–11464, http://dx.doi.org/10.1016/j.ijhydene.2015.01.097.

[22] H. Jorschick, A. Bulgarin, L. Alletsee, P. Preuster, A. Bösmann, P. Wasserscheid, Charging a liquid organic hydrogen carrier with wet hydrogen from electrolysis, ACS Sustain. Chem. Eng. 7 (4) (2019) 4186–4194, http://dx.doi.org/10.1021/acssuschemeng.8b05778.

[23] T. Rüde, A. Bösmann, P. Preuster, P. Wasserscheid, W. Arlt, K. Müller, Resilience of liquid organic hydrogen carrier based energy-storage systems, Energy Technol. 6 (3) (2018) 529–539, http://dx.doi.org/10.1002/ente.201700446.

[24] J. Vinoth, I.R. Young, Global estimates of extreme wind speed and wave height, J. Clim. 24 (6) (2011) 1647–1665, http://dx.doi.org/10.1175/2010JCLI3680.1.

[25] B. Molin, Offshore Structure Hydrodynamics, in: Cambridge Ocean Technology Series, Cambridge University Press, Cambridge, United Kingdom, 2023.

[26] J. Lippert, P. Wasserscheid, M. Geißelbrecht, Continuous hydrogenation of the hydrogen storage compound benzyltoluene in a trickle-bed reactor – influence of mass transfer and optimization strategies, Int. J. Hydrog. Energy 211 (2026) 153617, http://dx.doi.org/10.1016/j.ijhydene.2026.153617.

[27] H.Y. Tong, F.W. Karasek, Flame ionization detector response factors for compound classes in quantitative analysis of complex organic mixtures, Anal. Chem. 56 (12) (1984) 2124–2128, http://dx.doi.org/10.1021/ac00276a033.

[28] C. Greenshields, H. Weller, Notes on Computational Fluid Dynamics: General Principles, CFD Direct Limited, 2022.

[29] J. Brackbill, D. Kothe, C. Zemach, A continuum method for modeling surface tension, J. Comput. Phys. 100 (2) (1992) 335–354, http://dx.doi.org/10.1016/0021-9991(92)90240-Y.

[30] S.F. Kistler, Wettability, Vol. 6, 1993, pp. 311–430, Ch. Hydrodynamics of Wetting.

[31] R.M. Q.-F., R.J. Lopes, CFD modelling of multiphase flow distribution in trickle beds, Chem. Eng. J. 147 (2–3) (2009) 342–355, http://dx.doi.org/10.1016/j.cej.2008.11.048.

[32] C. Hirt, B. Nichols, Volume of fluid (vof) method for the dynamics of free boundaries, J. Comput. Phys. 39 (1) (1981) 201–225, http://dx.doi.org/10.1016/0021-9991(81)90145-5.

[33] S. Muzaferija, M. Peri'c, Computation of free-surface flows using the finite-volume method and moving grids, Numer. Heat Transfer B 32 (4) (1997) 369–384, http://dx.doi.org/10.1080/10407799708915014.

[34] J. Ferziger, M. Perić, R. Street, Computational Methods for Fluid Dynamics, Engineering, Springer International Publishing, 2019.

[35] H. Held, H. Freund, Identification of mass transfer limitations by kinetic modeling of a technical-scale trickle bed reactor for the hydrogenation of viscous aromatics, Ind. Eng. Chem. Res. 63 (1) (2024) 147–162, http://dx.doi.org/10.1021/acs.iecr.3c03273.

[36] C.-H. Yang, Y. Jin, A. Kan, Y. Wang, Y. Wu, J. Wang, Modelling and analysis of multiphysics transport processes in proton exchange membrane electrolysis cell under marine motions, Renew. Energy (2024) http://dx.doi.org/10.1016/j.renene.2024.122188.

[37] T. Liu, Z. Zhao, W. Tang, Y. Chen, C. Lan, L. Zhu, W. Jiang, Y. Wu, Y. Wang, Z. Yang, D. Yang, Q. Wang, L. Luo, T. Liu, H. Xie, In-situ direct seawater electrolysis using floating platform in ocean with uncontrollable wave motion, Nat. Commun. 15 (2024) http://dx.doi.org/10.1038/s41467-024-49639-6.

[1] Note that on the finest grid, the liquid took longer to 'find' its final channel than on the medium grid (20 s instead of 8 s).